DOI: 10.1111/cgf.12564
EUROGRAPHICS 2015 / O. Sorkine-Hornung and M. Wimmer
(Guest Editors)

Volume 34 (2015), Number 2

Content-Independent Multi-Spectral Display Using Superimposed Projections

Yuqi Li [1,2], Aditi Majumder[1], Dongming Lu[2] and M. Gopi[1]

[1]University of California, Irvine
[2]Zhejiang University, Hangzhou, China

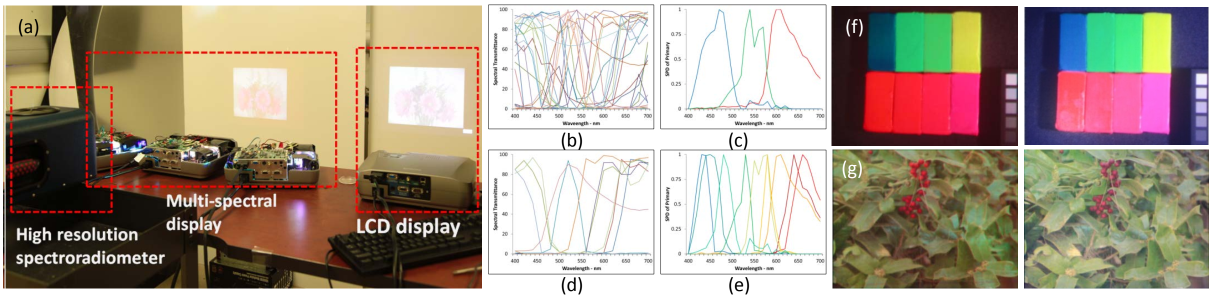

Figure 1: (a) Multi-spectral display system setup with three modified conventional 3-primary projectors, a conventional LCD 3-primary projector for comparison and a high spatial and spectral resolution spectroradiometer (SOC-730 hyperspectral camera) for measurements. (b)The candidate set of 30 primaries used for our prototype, (c) the existing *r*, *g* and *b* filters of the projectors, (d) the 9 filters chosen by our algorithm, (e) the 9-primaries generated by multiplying the *r*, *g* and *b* primaries with the 9 chosen filters. (f) and (g) show the results of our 9-primary multi-spectral display (left) when compared with a conventional 3-primary display (right).

Abstract

Many works focus on multi-spectral capture and analysis, but multi-spectral display still remains a challenge. Most prior works on multi-primary displays use ad-hoc narrow band primaries that assure a larger color gamut, but cannot assure a good spectral reproduction. Content-dependent spectral analysis is the only way to produce good spectral reproduction, but cannot be applied to general data sets. Wide primaries are better suited for assuring good spectral reproduction due to greater coverage of the spectral range, but have not been explored much.

In this paper we explore the use of wide band primaries for accurate spectral reproduction for the first time and present the first content-independent multi-spectral display achieved using superimposed projections with modified wide band primaries. We present a content-independent primary selection method that selects a small set of n primaries from a large set of m candidate primaries where $m > n$. Our primary selection method chooses primaries with complete coverage of the range of visible wavelength (for good spectral reproduction accuracy), low interdependency (to limit the primaries to a small number) and higher light throughput (for higher light efficiency). Once the primaries are selected, the input values of the different primary channels to generate a desired spectrum are computed using an optimization method that minimizes spectral mismatch while maximizing visual quality. We implement a real prototype of multi-spectral display consisting of 9-primaries using three modified conventional 3-primary projectors, and compare it with a conventional display to demonstrate its superior performance. Experiments show our display is capable of providing large gamut assuring a good visual appearance while displaying any multi-spectral images at a high spectral accuracy.

Categories and Subject Descriptors (according to ACM CCS): I.3.3 [Computer Graphics]: Picture and Image Generation—Display Algorithms; I.3.7 [Computer Graphics]: Three-Dimensional Graphics and Realism—Color; I.4.0 [Image Processing and Computer Vision]: Image Displays—;

1. Introduction

A spectrum is the distribution of light radiance intensity at different wavelengths. Multi-spectral data can be acquired today at a relatively high spatial and spectral resolution creating what is commonly known as multi-spectral images. Many methods have been proposed to acquire, compress, and analyze multi-spectral images. However, displaying multi-spectral images is still a challenging task.

Conventional RGB display uses only three spectral bands - red, green and blue. Multi-spectral images contain far more spectral bands than these three and hence displaying a multi-spectral image on a RGB display would result in significant loss of information. Further, the norm is to consider one representative human response to colors and try to make the three primaries in a RGB display as close as possible to the spectral sensitivity functions of the CIE standard observer so that it can be assumed that the lost information is not perceived by the humans. However, [SB59, KR04, IIN*01] showed that in reality the three spectral sensitivity functions in humans can vary significantly across different individuals, especially when considering factors like age, race and eye fatigue – a previous measurement experiment [AF97] with twenty individuals has show that the maximum inter-observer perceived CIE Lab color difference is two times larger than the maximum color discrimination threshold of an individual observer. This variance can be even higher when considering different human eye conditions like color blindness and hypochromatopsia or even different man-made imaging systems including cameras. Thus two significant different spectra result in colors that are match for one observer, but may unacceptable match for another (observer metamerism). Conventional three primary displays do not aim to reproduce the exact spectrum, but an acceptable metameric spectrum as perceived by the CIE standard observer. Thus, it only produces a low fidelity approximation of the real spectrum which is not correct for any observer or capture device (Figure 9).

In this paper we present a new content-independent multi-spectral display that can display multi-spectral images as accurately as possible by minimizing the spectral difference between the displayed and the desired spectrum while maximizing the visual quality. Such a display can produce high fidelity perception for all observers and capture devices, independent of the number of spectral channel they have and their sensitivities. Observer metamerism is an unavoidable fundamental limitation of colorimetry, closer spectral reproduction can effectively reduce the color mismatch caused by various observers with different ages and different viewing angles [FW07]. The key aspect we explore in achieving this is the use of wide band primaries. We choose a set of n ($n > 3$) wide-band primaries that minimize our content-independent objective function. It is evident that wide primaries would facilitate greater accuracy in spectral reproducibility by the sheer advantage of having a better coverage of all the visible wavelengths and smooth spectral power distribution [BL07]. When using a fixed number of primaries, a display using wide-band primaries is more light-efficient than the one using narrow-band primaries. It also has less observer metamerism. However, wide primaries may provide a smaller CIE color gamut and out-of-gamut spectrum display can cause large perceived color difference in perception of individual observers. These put contradictory demands on the selection of primaries for a general multi-spectral display. Instead of selecting primaries in an ad-hoc manner, we take into account the human visual sensitivity and present a new primary selection method that carefully considers light throughput, gamut and spectral reproduction. We use the completeness of coverage as a simple and intuitive guideline to decide the primaries in the trade-off and guarantee a high light throughput. These primaries are realized by using filters on conventional RGB projectors that change the original spectra of its primaries. Multiple such projectors with superimposed field-of-projection are then used to create the multi-spectral display. Thus, to create n primaries, we need to superimpose $\lceil \frac{n}{c} \rceil$ c-primary projectors.

1.1. Main Contributions

We present a *content-independent* multi-spectral display via superimposition of multiple projectors that strives to maximize the image quality. The main contributions of our work are as follows.

1. We present the first content-independent primary selection method that can maximize the quality of the multi-spectral display without prior knowledge of multi-spectral data set. Given the possible set of primaries and the number of required primaries, our method would select the best possible primaries within that constraint. Unlike earlier methods that focus on enlarging gamut and color reproduction, our multi-spectral display chooses primaries from adequate number of wide-band candidates to provide a good spectral reproduction without significantly compromising the color gamut. As the number of chosen primaries increases, the quality of the multi-spectral display would be improved. We also show empirically that beyond a certain number the benefits stagnate.
2. Given the selected set of primaries, we propose an optimization method to compute the intensity of each primary required to achieve a desired spectrum. Our algorithm minimizes a well-designed objective function that minimizes both spectral and perceptual error. This algorithm can achieve near interactive capabilities by exploiting the temporal coherence of a multi-spectral image sequence and the parallelism offered by GPUs.
3. We implement a practical multi-spectral image display prototype using superposition of modified primaries from three projectors. Experimental results from this prototype

demonstrate significantly higher quality of this display when compared to a conventional RGB display.

2. Related Works

There have been many recent efforts to study multi-spectral displays for accurate color and/or spectral reproduction [MWDG13]. The techniques pursued can be classified into two categories: *spectral modulation* and *multi-primary display*.

Spectral modulation techniques split the white wide-band illumination spectrum to create multiple narrow-band illumination channels. The radiometric intensity of each of these channels is then spatially modulated using a spatial light modulator panel (e.g. DMD array). [RBA*12] developed a multi-spectral projector system which can produce arbitrary spectrum by adopting such a spectral modulation. However, implementation of such a system involves large-scale modification of the light source of the projector by using precise laboratory optical components. In order to simplify the design, [MRT08] proposed an agile spectrum projector that swapped the order of spectral modulation component and spatial modulation component on the optical path enabling the spectral modulation module to be placed outside an unchanged conventional projector. However, this requires long optical path and may bring obvious chromatic artifacts if it is out of focus. These render the projection display inflexible since the distance and pose of the projection becomes fixed and can only project on flat surfaces.

Multi-primary displays with more primaries than conventional 3-primary displays have become popular as an emerging display technology to produce larger color gamut and hence better color reproduction. [AOYO99] generates multiple narrow primaries by using a diffraction grating and a liquid crystal panel. [RC05] uses three bandpass interference mirrors to disperse light and add an extra yellow channel to an RGB projector to develop a 4-primary projector prototype. More primaries can be added to such systems easily with little optical modification by adding projectors. [AOYO00] and [YTO*02] manually use long-pass filters and short-pass filters to modify the RGB channels of two projectors differently to synthesize a 6-primary color-reproduction display. However, larger color gamut is only possible via narrow band primaries that produce more saturated primaries [RPSF14]. Hence, aforementioned works use narrow band primaries, sometimes specially engineered to provide other benefits like high brightness, power-savings and resolution [TYN*12]. However, such multi-primary displays are not necessarily multi-spectral displays. Narrow band primaries provide a large color gamut, but provide limited coverage of the entire set of visible wavelengths in a broad-band spectrum. Hence it cannot achieve accurate spectral match, but only a metameric match which is acceptable for only the CIE standard observer and not for various individual observers. Thus, these displays are merely multi-primary displays and not multi-spectral displays.

Multi-spectral displays, whose primary consideration is accurate spectral reproduction and not just an increased color gamut, have used content dependent primary selection. [BCE07] uses a non-negative matrix factorization (NMF) and singular value decomposition (SVD) to choose the appropriate primaries that can preserve the spectral quality of a specific hyperspectral image. [LF11] shows in simulation that selecting six optimized Gaussian shaped primaries can significantly improve spectral reproduction for a specific image or a small set of images. However, being content dependent, these methods imply an unrealistic demand of needing to change the primaries every frame which is unacceptable for a temporally continuous display.

3. Multi-Primary Multi-Spectral Display Design

Our multi-primary multi-spectral display design has three core parts. First, we choose appropriate primary spectra that would sufficiently cover any desired arbitrary spectrum (Section 3.1). Second, given the spectra of the primaries and the desired spectrum, we compute the intensity of each primary at which it has to be projected and combined to match the desired spectrum (Section 3.2). Finally, we design and implement a prototype multi-primary multi-spectral projection display (Section 3.3) that uses the above techniques to display any arbitrary multi-spectral image(s) at near interactive rates.

3.1. Content-Independent Multi-Primary Selection

Let us consider an n-primary multi-spectral display where the spectrum of the primaries are given by $\{p_1(\lambda), p_2(\lambda), \ldots p_n(\lambda)\}$, where $p_i(\lambda)$ is the intensity of the ith primary at wavelength λ in the visible spectrum, i.e. $400nm \leq \lambda \leq 700nm$. For simplicity, in this paper, primary p_i represents the combination of projected spectrum of primary i and spectral reflectance of projection screen.

From the given set of m primaries, which we call the candidate primaries, we seek the above set of n primaries $(n > 3)$ that can be used to adequately approximate most of the general spectra available in nature and in man-made objects. These chosen primaries are then used to create the different channels in multiple superimposed projectors to achieve the multi-primary display. Following such a selection, for any general spectrum $l(\lambda)$, we can find the weights $\alpha_i > 0$ such that the weighted sum of these primaries is close to $l(\lambda)$, i.e. $\sum_{i=1}^{n} \alpha_i p_i(\lambda) \approx l(\lambda)$. This process is detailed in Section 3.2.

A large number of inexpensive off-the-shelf broad-band filters are available online along with their specifications as in `http://www.rosco.com/filters` and `http://www.internetapollo.com/Products/Group/`

`Dichroic+Filters.aspx`. Choosing 9 primaries from such a set of 70 candidate primaries yields $C(70,9) = 6.5 \times 10^{10}$ possible combinations. Naive exhaustive methods to select primaries is NP-hard and imprатical. The well known NP-hard column subset selection problem can be reduced to our primary selection problem. In order to address this problem, first we reduce the set of candidate primaries by eliminating those that do not have the required characteristics to be in a multi-spectral system. Then we cluster the set of candidate primaries and choose one primary from each cluster that would be eventually used in the multi-spectral projection system.

3.1.1. Desired Characteristics of the Chosen Primaries

We evaluate a combination of primary filters using three selection criteria – high light throughput, completeness of coverage, and low inter-dependency. Note that the candidate filter our method uses are wide-band and have smooth spectral transmission function.

High Light Throughput: Low light throughput typically leads to relatively higher energy loss during filtering. Hence, to assure a good quality display we first discard primaries with very low light throughput from the candidate list. We define the light throughput of a primary p_i as the integral spectrum values over all wavelengths $\int_\lambda p_i(\lambda)\, d\lambda$, but for computational simplicity, we use the peak intensity value of spectrum $max(p_i(\lambda))$ as an indicator of the light throughput (only for wide-band primary).

Completeness of Coverage: Accurate spectral reproduction means we need to create an exact match in the power at every wavelength. So, the presence of each and every wavelength in the primaries is critical to achieve a good spectral match. This is the primary motivation behind our choice of wide-band filters contrary to conventional practice of choosing narrow band filters that are used to increase the color gamut of a display. Therefore, we are guided by the principle that all our primaries together should cover the entire range of visible wavelengths without leaving any "gaps".

In order to define coverage of a spectrum we use the concept of Full-Width at Half-Maximum (FWHM) that measures the coverage of a spectrum as the range of wavelengths where the spectrum has more than half its maximum intensity. Recently, this measure has been used to represent the primary coverage in order to evaluate the possibility of observer metamerism in displays [Ram09]. We propose a more general form of the FWHM metric which we call the Range at Weighted-Maximum (RWM) to accommodate multi-modal spectrum. RWM of a spectrum is measured as all the ranges of wavelength that are covered at w times the maximum intensity where $0 < w < 1$ (Figure 2). The weight w also serves as one of the parameters for our optimization (Section 3.2). Completeness of coverage is guaranteed by assuring that the union of the RWM of all the primaries covers all the wavelengths in the visible spectrum,

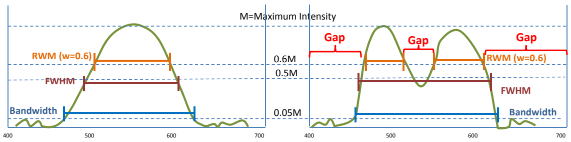

Figure 2: The figure illustrates the computation of the bandwidth (blue), full bandwidth at half maximum (red) and range at weighted maximum (orange) for two different spectra – a single lobed and a multi-lobed one. Note that the bandwidth defined by RWM is suitable for measuring the coverage and gaps of multi-modal spectrum accurately.

i.e,

$$\cup_i RWM(p_i) = \{\lambda | \lambda \in [400, 700]\} \tag{1}$$

Low Inter-Primary Dependency: The only way to minimize the number of chosen primaries, and at the same time satisfy completeness of coverage is to choose wide band filters. Further, to maximize the set of output spectra that can be synthesized using this set of n wide band primaries, we need to choose primaries that are complementary and hence are not highly correlated with each other. We define the dependency between primary p_i and p_j using a common similarity metric used in spectral clustering [TMGR10] – the Gaussian weighted Euclidean distance, d_{ge} defined as

$$\begin{aligned} d_{ge}(p_i, p_j) &= exp[-\frac{\sum_\lambda (\hat{p}_i(\lambda) - \hat{p}_j(\lambda))^2}{\delta^2}] \\ where \quad \hat{p}_k(\lambda) &= \frac{p_k(\lambda)}{max(p_k(\lambda))} \quad (k = \{i, j\}) \end{aligned} \tag{2}$$

and δ is the standard deviation of the spectral power distribution of all the candidate primaries. High values of d_{ge} represent high inter-primary dependency. Using the above similarity metric we first cluster the given set of candidate primaries such that the spectra within a cluster has high dependency, and inter-cluster spectra have low dependency. We pick no more than one spectrum from each cluster to ensure low inter-primary dependency among the final chosen set of primaries. Obviously, if the primaries are narrow band their inter-dependency will be low. However, we would need many such narrow band primaries to satisfy the primary coverage completeness of the entire visible range. So in our primary selection algorithm (Section 3.1.2) we first start with narrowest band primaries within each cluster (which also assures large color gamut), and if there is any gap in the visible spectrum that is not covered, we replace the narrow band primary with progressively broader band primary from the same cluster until the gap is covered.

The above guidelines provide us a set of high light throughput relatively wide band filters which are at the same time narrow enough to have low inter-dependency. Such a set of filters will not be able to reproduce spectra with very sharp variations. However, previous works have shown that both man made and natural objects or phenomena have smooth spectral reflectance [Dan92], and sunlight and many man made light source have smooth-shaped spectra [CCO00]. It has also been shown that the dimensions of spectral basis functions required to represent them can be easily reduced to 8-10 wide-band spectra. This provides a strong hope that even with the small number of selected wide-band primaries we can reproduce a large number of general spectra. Fortunately, as a side effect, wide-band filters also assure greater light efficiency and throughput resulting in the added advantage of an energy-efficient display.

3.1.2. Primary Filters Selection Algorithm

Algorithm 1 Multi-Primary Selection

Input: Set of candidate primaries: $\{q_j(\lambda)|j = 1,\dots,m\}$.
Input: Number of output primaries: n
Output: Selected set of n primaries: $\{p_i(\lambda)|i = 1,\dots,n\}$.
1. Discard the primaries with light throughput below a certain threshold and use the remaining m', $m' < m$, primaries;
2. Spectral clustering: Partition $\{q_j|j = 1\dots m'\}$ into $k \geq n$ clusters;
3. Define the RWM of each primary;
4. Choose n clusters C_i $(1 \leq i \leq n)$, with narrowest average RWM;
5. Select the primary $\{p_i|i = 1,\dots,n\}$with narrowest RWM in each cluster C_i;
6. Find the set of gaps G where each gap $g \in G$ is a continuous range of wavelength not in $\cup_i$ RWM(p_i);
repeat
  for all $g \in G$ **do**
    7. p_k = the closest primary to g;
    8. Use the primary with the next wider bandwidth in the cluster of p_k to replace p_k;
  end for
  9. Update G;
until $\cup_i$RWM$(p_i) = \{\lambda|\lambda \in [400,700]\}$.
return n primaries $\{p_i(\lambda)|i = 1,\dots,n\}$;

In this section, we describe our method to select the set of most appropriate n primaries from the m candidate primaries set (Algorithm 1). First, we discard all the primaries with light throughput below a certain threshold to give us m' primaries where $m' < m$. Next, we perform a spectral clustering to divide the m' candidate primaries into k $(k >= n)$ dispersedly distributed clusters using the spectral clustering method in [BJ04]. In this method, first a similarity matrix S with $S(i,j) = d_{ge}(p_i, p_j)$ (Equation 2) is defined to denote the similarity between primary p_i and p_j. Next, a normalized cut is used to achieve the spectral clustering. This method of spectral clustering has been shown to be efficient at spectral classification and hyper-spectral images segmentation in earlier works [TMGR10].

The clustering assures that primaries in the same cluster have similar spectral distributions while those in different clusters have lower inter-dependency. We then sort these k clusters in increasing order of the average RWM of the primaries belonging to the cluster, and choose the first n clusters. Ideally, bandwidth is defined as the range of wavelengths in which the spectrum has positive intensity. However, to nullify the effect of noise, we consider the bandwidth to be the RWM at $w = 0.05$ (Figure 2).

From these n clusters, one primary from each cluster that has the narrowest bandwidth is chosen. This assures that each of the selected primaries have high saturation and low dependency on each other. This in turn assures a relatively larger gamut in CIE color space, and the number of spectra for which these primaries can reproduce the metamers is relatively large. Next, in order to assure that these primaries also cover all the wavelengths in the visible range, we find the gaps in the coverage of the selected n primaries i.e. the range of frequencies that is not covered by any primary. In order to reduce or remove this gap, we replace either or both the primaries adjacent to the gap by other primaries within their same cluster but with wider RWM. The primary whose maximum intensity is at a wavelength closest to the center of the gap is changed first. This process continues until all the gaps are covered. If the gaps are not covered, we repeat the entire process with a smaller value of k.

Figure 3 shows the entire pipeline of our primary selection process. We show 30 candidate primaries. First they are divided into 12 clusters. Our goal is to choose six primaries. Note how the gamut changes as the selection of primaries change. Also, note that the gaps in the coverage are removed at the end of the primary selection process.

Note that our algorithm does not strive to achieve an optimal solution for this NP hard problem. We choose w to be between 0.4 and 0.6 when finding RWM. We run the spectral clustering algorithm for different values of k between $1.5n$ and $2n$ and from each such clustering choose the n primaries using our Algorithm 1. Out of these multiple choices of n primary sets, the one with the highest intensity primaries is chosen as the final result. Exploring the spaces spanned by the different design choices (for e.g. choosing the top n clusters based on the number of primaries in them instead of their narrowest average RWM, choosing k based on the standard deviation of the the RWMs of the primaries in a cluster) to find an optimal solution is an interesting theoretical problem and can only improve multi-spectral display design in the future.

3.2. Displaying Multi-Spectral Data

Let the desired spectrum to be displayed at a particular pixel be $l(\lambda)$. In this section, we describe how we compute the contribution $\alpha_i (0 \leq \alpha_i \leq 1)$ from each selected primary p_i such that their weighted sum is as close as possible to the desired spectrum $l(\lambda)$ closely. The distance between the reproduced and desired spectra can be computed either in the spectral space or in the perceptual space (CIE XYZ color space). Previous work [IRB02] shows that the selection of metrics should be made based on appropriateness to applications, neither spectral difference metric nor perceptual

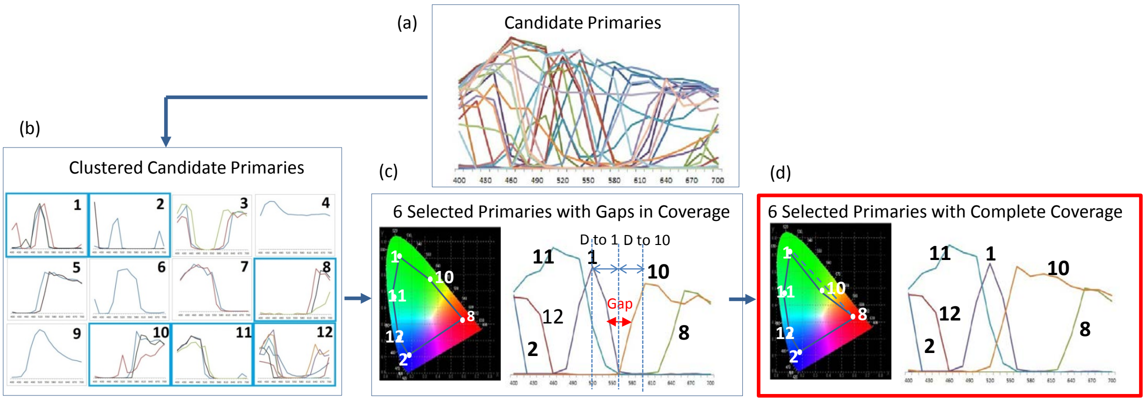

Figure 3: In this figure we start with $m = 30$ candidate primaries (a) and choose six out of them (d). First, we cluster the primaries into 12 groups (b). We highlight in blue the first six groups when sorted based on the average bandwidth of the primaries in the group. (c) shows the initially chosen 6 primaries that have the narrowest bandwidth in each of these clusters. However, this creates gaps in the coverage. Clusters 1 and 10 are adjacent to the gap in which the center of cluster 10 is closer to the center of the gap. So, a wider primary from cluster 10 is chosen to replace the earlier chosen primary (d). (c) and (d) also show how the gamut of the display shrinks slightly as we go from the initial choice of narrow primaries to the final wider primaries. However, this results in better spectral approximations.

difference metric consider both human vision and observer metamerism which are two important issues in our display application. Thus we use a weighted combination of both these distance metrics to compute the error between the reproduced and desired spectra. The values of α_i are those that minimize this error.

Spectral Error: The spectral error E_s is the error of the reproduced spectrum from the original spectrum and is defined as

$$\triangle E_s = \int_\lambda (\sum_{i=1}^{N} \alpha_i p_i(\lambda) - l(\lambda))^2 d\lambda \tag{3}$$

The discretized form of the above equation can be rewritten in matrix form as

$$\triangle E_s = (PA - L)^T (PA - L) \tag{4}$$

where P is a $t \times n$ matrix, t is the number of spectral bands used, A is a $n \times 1$ column vector of α_i and L is a $t \times 1$ vector representing the desired spectrum. Here, we ignore black offset of projectors since it is invisible to our hyper-spectral camera.

Perception Error: The spectral error function gives equal importance to the errors in all wavelengths. On the other hand, for a good perceptual match (metamers) and hence for a good visual quality of the display, reproducing the spectrum with very low error at certain wavelengths is more important than at other wavelengths. In other words, a good spectral match does not always ensure a good perceptual match or vice versa. In order to compute the perceptual error function, we consider CIE 1964 10° standard observer as a representative observer for reasons explained later in the section. We first compute the tristimulus values for the desired spectrum $l(\lambda)$, (X_0, Y_0, Z_0), and for all the primaries $p_i(\lambda)$, (X_i, Y_i, Z_i) using the color matching functions of this observer. We define the perception error as

$$\triangle E_p = (X_0 - \sum_{i=1}^{n} \alpha_i X_i)^2 + (Y_0 - \sum_{i=1}^{n} \alpha_i Y_i)^2 + (Z_0 - \sum_{i=1}^{n} \alpha_i Z_i)^2 \tag{5}$$

If the desired spectrum is in the gamut of the multi-primary display, the corresponding color error $\triangle E_p$ would be 0; otherwise, the minimization of $\triangle E_p$ would map (X_0, Y_0, Z_0) to the nearest coordinate (X', Y', Z') which is in the gamut of the multi-primary display (Figure 3). This can be written in matrix form as

$$\triangle E_p = (\begin{bmatrix} X \\ Y \\ Z \end{bmatrix} A - \begin{bmatrix} X_0 \\ Y_0 \\ Z_0 \end{bmatrix})^T (\begin{bmatrix} X \\ Y \\ Z \end{bmatrix} A - \begin{bmatrix} X_0 \\ Y_0 \\ Z_0 \end{bmatrix}) \tag{6}$$

where X, Y, and Z are $1 \times n$ vectors of X_i, Y_i and Z_i respectively. A is the vector of α_is as defined before.

Choice of Representative Observer: CIE standard observer color matching functions were constructed by averaging measured responses of several individual observers. Therefore, although observer variance exists, color-matching-functions of individual observers distribute around those of the standard observer. Hence, to compare the visual quality of a display, minimizing the difference in perception of a standard observer is a reasonable way to minimize difference in perception across various different observers. Several such standard observers have been defined – for example 1931 2° standard observer, 1964 10 ° standard observer and so on. We choose CIE 1964 10° standard observer since the field of view in our application is generally larger than 5° and the response is linear which enables fast optimization required for interactive rendering.

Objective Error Function: The complete objective function to compute the error therefore consists of the weighted sum of spectral error $\triangle E_s$ and perception error $\triangle E_p$ and is given by

$$\triangle E = \triangle E_s + s^2 \triangle E_p$$
$$= (\begin{bmatrix} P \\ sX \\ sY \\ sZ \end{bmatrix} A - \begin{bmatrix} L \\ sX_0 \\ sY_0 \\ sZ_0 \end{bmatrix})^T (\begin{bmatrix} P \\ sX \\ sY \\ sZ \end{bmatrix} A - \begin{bmatrix} L \\ sX_0 \\ sY_0 \\ sZ_0 \end{bmatrix}) \quad (7)$$
$$s.t. \quad \alpha_i \geq 0 \quad (i = 1, \ldots n),$$

where s is used to control the relative contribution of spectral and perception error. The weight s is squared for convenient representation. As shown in Table 1, we use perceived color difference of a Stiles-Burch observer to illustrate the trade-off between perception error term and spectral error term. The Stiles-Burch observer is obtained from ten measured 2° Stiles-Burch individual observers and it is little different from the CIE 1964 standard observer. Here we use the Stiles-Burch observer as a benchmark to evaluate observer metamerism, thus less perceived color difference represents less observer metamerism exists in the display. With no perceptual error term we indeed get the best spectral reproduction but large errors in CIE observer perception, but when S^2 is increased, the CIE perceptual errors are significantly reduced but the spectral accuracy is compromised negligibly. However, the Stiles-Burch perceptual error (observer metamerism) has a minimum value when S^2 is between 1 and 100. Thus we use S^2 in the range of 1 to 100 in our experiments.

	S^2					
Error	0	1	10	100	1000	∞
CIE1964	2.600	0.952	0.081	0.001	0	0
Stile-Burch	2.410	0.952	0.843	0.909	0.910	0.910
Spectrum	21.33	22.69	23.82	23.98	23.99	23.99

Table 1: Mean perceptual color difference $\triangle E_{Lab}$ of CIE standard observer and a Stiles-Burch observer [PMaH97] between desired color and simulated color and spectral difference for displaying spectrum in a spectral dataset using our optimization with varied S^2 values. Note that the perceived color difference of the Stile-Burch observer exists an extreme at $S^2 = 10$. The primary combination used here is the chosen primaries in Figure 3. The test spectral dataset is the 2538 spectrum used in Figure 9.

We seek α_i that would minimize $\triangle E$. However, note that $\alpha_i \geq 0$ to avoid negative light as solution. We use a fast non-negative least squares (NNLS) algorithm [BJ97] to minimize the objective function. This assures non-negative values for α_i. To enforce the upper bound of 1 on the α_i, we normalize its value across the entire multi-spectral image, as $\bar{\alpha}_i(x,y) = \frac{\alpha_i(x,y)}{max(\alpha)}$ where (x,y) is the spatial coordinates of a pixel and $max(\alpha)$ is the maximum value of $\alpha_i(x,y)$ over all i and all values of x and y. This normalization compresses brightness of output spectrum into capacity range of our multi-spectral display while preserving the shape of the desired spectrum. Since the computation of α_i for each pixel is independent of each other, it can be parallelized in GPU using the fast non-negative least square method.

3.3. Prototype Design

In this section we present a prototype design and implementation of a multi-spectral display using multiple existing projectors (Figure 1).

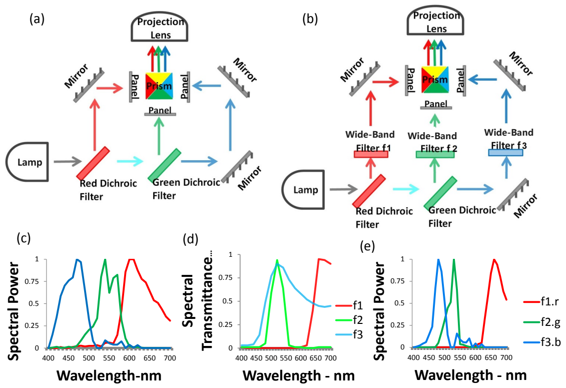

Figure 4: Modified projector (b) by adding three filters on the optical path of three primaries of a ordinary LCD RGB projector (a). The three existing primaries of the projector (c) are modified by the filters f_1, f_2 and f_3 (d) to create the modified filters $f_1 \odot r$, $f2 \odot g$ and $f_3 \odot b$ (e).

In order to create an n primary display using conventional 3-primary projectors, we need $\lceil \frac{n}{3} \rceil$ projectors. Each primary of each projector is modified to create a different primary and the projections from the $\lceil \frac{n}{3} \rceil$ projectors are then superimposed to create an n primary display. Replacing original filters on the color wheel of DLP projector or replacing the three color filters on an LCD projector is the direct method to create new primaries. In the case we can apply our primary selection method directly. However, removing the filters is practically impossible in any existing projector hardware where these filters are custom manufactured and well integrated with the optics of the projector. Instead we insert new filters on the illumination path for each channel to create our new primaries whose spectral response is now the product of that of the existing projector filter and the newly inserted filter. Figure 4 shows the design. Here filters $f_1(\lambda)$, $f_2(\lambda)$ and $f_3(\lambda)$ are placed on the path of the red, green and blue light respectively to create the three new and different primaries. Figure 4 also shows the spectrum of the original projector primaries $r(\lambda)$, $g(\lambda)$ and $b(\lambda)$, the spectrum of the new filters $f_1(\lambda)$, $f_2(\lambda)$ and $f_3(\lambda)$, and the new primaries resulting due to their componentwise multiplication given by $f_1(\lambda) \odot r(\lambda)$, $f_2(\lambda) \odot g(\lambda)$ and $f_3(\lambda) \odot b(\lambda)$. To select filters for this prototype, the selection method need to be adjusted.

Assume that we are using the same brand projectors and hence their red, green and blue channel spectra are identical and given by $r(\lambda)$, $g(\lambda)$ and $b(\lambda)$. Let us also assume that we have m different external filters with spectra $f_i(\lambda)$ available to intercept the light path of each channel. Our possible choice of primaries is not the spectra of new filters f_i, but are $f_i(\lambda)\odot r(\lambda)$, $f_i(\lambda)\odot g(\lambda)$ and $f_i(\lambda)\odot b(\lambda)$ $\forall i, 1 \leq i \leq m$. Nevertheless, multi-spectral projector with any n primaries chosen from this list of $3m$ primaries is not a feasible solution, since for each projector we need three primaries of the form $f_i(\lambda)\odot r(\lambda)$, $f_j(\lambda)\odot g(\lambda)$ and $f_k(\lambda)\odot b(\lambda)$. Hence we need to consider each projector as a single unit (three filters add up to create a single spectrum) and the number of different possible sets of three primaries that we can generate is given by the permutation of the m primaries in the three channels, $M = m^3$ (assuming repeatability of filters). Each of these permutations represents the chosen three filters and its corresponding channels that these filters go into for a single projector.

Given that we need $\lceil \frac{n}{3} \rceil$ projectors to create an n primary system, our goal is to use our primary selection method described in Section 3.1.2 to choose $\lceil \frac{n}{3} \rceil$ primaries from these M candidate primaries where the spectrum of each candidate primary (each permutation) is given by the addition of its three spectra. The output of the primary selection algorithm gives, for each projector, the choice of external filters and the channels in which they need to be placed.

The multi-spectral display is then created by superimposing the projections on a planar display from the $\lceil \frac{n}{3} \rceil$ projectors which are aligned non-coaxially with different distance and different pose. This can cause geometric and photometric misregistrations. Since the projection screen is planar in our prototype, we register the multiple superimposed projections using standard homographies [SSM01] to achieve geometric registration. To achieve color-seamlessness, we use Bezier surfaces to smooth brightness across the display [SLGM09]. Unlike spectral modification methods, our system can also be used on non-planar surfaces with appropriate geometric registration [SM09, SM10, SM11, DYA*12].

4. Implementation and Results

We have implemented our method both in simulation and in a real prototype. We use a database of around 60 multi-spectral images. Twenty-eight of these were captured using a SOC-730 hyperspectral camera at a spatial resolution of 1024×1024 and spectral resolution of $t = 31$ of using $10nm$ wide spectral bands. The rest are taken from the CAVE database of hyperspectral images from `http://www.cs.columbia.edu/CAVE/databases/multispectral/`. For our primaries we use the inventory of 70 available filters from Rosco and Apollo. Our primary selection program is written in matlab. Our implementation of fast-non-negative least square algorithm for input calculation for displaying a 800×600 multi-spectral image with 31 spectral bands and 9 primaries on Nvidia Quadro 6000 runs

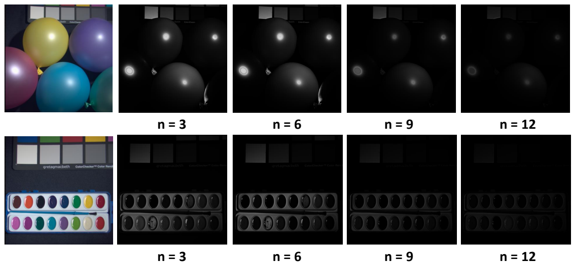

Figure 5: This figure shows our primary selection method on some multi-spectral image. The error is calculated at every pixel using our objective function (Equation 7) and then visualized as normalized gray scale images. As the number of primaries increase, the error progressively decrease assuring a closer spectral match.

at near interactive rates of 5 fps. This shows that displays for general multi-spectral video are possible in the near future.

We compute the error (Equation 7) for every image in our multi-spectral image database. Figure 5 shows that the error (Equation 7) progressively reduces as the number of primaries increases indicating a progressively more accurate spectral match to our multi-spectral image.

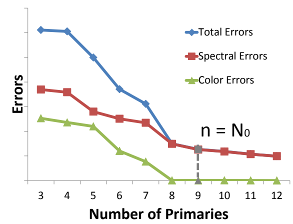

Figure 6: This shows that how the average error across all pixels across all images decrease with increase in number of primaries. Note that for $n > N_o$ the spectral error does not decrease while perception error becomes 0. This shows that increasing the primaries beyond N_o does not provide any added benefits.

In order to find the generality of the chosen primaries, in Figure 6 we plot against the different number of primaries, the average error over all pixels and all images in our database. Note that for $n > N_o = 9$, the error does not change at all indicating no improvement in spectral approximation with increasing number of primaries. This provides us with the empirical upper bound on the number of primaries needed to display multi-spectral images. Note that this confirms the results from [Dan92, CCO00] that shows that the dimensions of spectral basis functions required to represent most natural and man-made objects can be reduced to 8-10 wide-band spectra.

Comparison of other primary selection methods versus our method: Finding the optimal solution of the primary selection problem is impractical. Prior works exist on selecting non-optimal primaries to increase the color gamut of a display. To evaluate our selected primaries combination, we compare our method with a gamut-enhancing selection (GES) strategy and a previous filter selection method [CYBE10]. In the gamut-enhancing selection method, we first remove the low light throughput primaries as Algorithm 1 does, then we greedily choose the primary which can create the largest color gamut (in CIE 1964 xy chromaticity diagram) with previous selected primaries combination in each iterative step. Chi's method finds the optimal combination of primaries by minimizing an objective function which is the sum of the condition number of matrix P and the weighted reciprocal of the total light transmittances of primaries. We choose 6, 8, and 10 primaries from the set of 70 candidates using these three methods whose results are shown in Figure 7 and use these primaries to approximate our multi-spectral images by adapting the optimization in Section 3.2. To quantify the fidelity of the display with different primaries, we compare the CIE 1964 observer perceived error, a Stile-Burch observer [PMaH97] perceived error and spectral error (Table 2). Note that while GES method shows slightly less errors than our primary selection method for the CIE 1964 observer, it shows significantly higher Stiles Burch observer and spectral error. This is expected since the GES method is geared towards reducing standard observer error while Stiles Burch and spectral error stems from inaccurate spectral match. It is important to note that our primary selection process while keeping the CIE observer errors pretty close to that provided by the GES method, also reduces the spectral and Stiles Burch observer error significantly. This proves that our selected primaries can assure a large gamut while providing a close spectral reproduction. Chi's method endeavors minimum condition number which cannot ensure large gamut and close spectral approximation, thus the method gives worst perceived color difference of CIE observer and Stiles-Burch observer (Table 2).

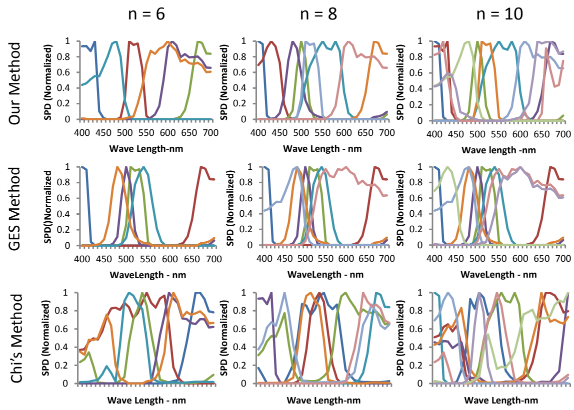

Figure 7: Spectral power distribution of selected primaries using our method (upper row), gamut-enhancing method (middle row), and Chi's method (bottom row). The primaries are normalized to 0-1 range. Note that the selected primaries of our method cover the whole wavelength range and distribute more dispersedly than those of other two methods. Further, the primaries chosen by our method have high light throughput without any deep gap between the primaries.

Multi-Projector Prototype: We also built a real prototype

		Error					
		CIE 1964		Stiles-Burch		Spectrum	
	n	mean	std	mean	std	mean	std
Ours	6	0.004	0.002	1.102	3.859	21.7	14.0
	8	0.001	0.001	0.947	4.189	20.4	13.4
	10	0.001	0.001	0.677	2.611	15.6	11.7
GES	6	0.004	0.006	6.687	14.79	472	513
	8	0	0	1.900	5.784	57.8	73.5
	10	0	0	0.997	4.237	27.2	21.4
Chi's	6	2.33	5.02	2.45	3.22	35.2	37.2
	8	0.032	0.067	1.79	1.55	38.5	37.7
	10	0.269	0.823	1.01	0.897	30.3	22.0

Table 2: Mean perceptual color difference $\triangle E_{Lab}$ of CIE standard observer and Stiles-Burch observer between desired color and simulated color and spectral difference for multi-spectral display using 6, 8, 10 primaries which are selected by our selection method, gamut-enhancing method and Chi's method.

of a 9-primary display by superimposing images from three conventional 3-primary projectors. Figure 1 shows an image of our setup and the prototype. We modified the projector using methods explained in Section 3.3. We used $m = 30$ Rosco filters which led to $M = 27,000$ different combined spectra of these filters with the red, green and blue filters of the projectors. We use our primary selection process to select three primaries from this. This takes around 30 seconds. The additional filters on the paths of the 9 different channels thus found are *PrimaryRed*, *FlameRed*, *MediumPink*, *Orange*, *Amber*, *PrimaryGreen*, *GaslightGreen*, *DeepPurple*, *DeepMagenta*. The spectra of these nine filters and the resulting new primaries are shown in Figure 1.

Comparison with Conventional LCD Projector: On any conventional 3-primary display (CD), the standard way to reproduce a desired spectrum $l(\lambda)$ is as follows. The input values to create the spectrum is generated with the goal of creating a metamer of $l(\lambda)$ rather than a spectral match. Hence, first the (X_l, Y_l, Z_l) corresponding to $l(\lambda)$ is computed using a CIE standard observer (we use CIE 1964 10° standard observer). Let us assume that the XYZ values corresponding to the maximum intensity red, green and blue primaries are given by (X_c, Y_c, Z_c), $c \in \{r, g, b\}$. Then the input R, G and B are computed from the relationship

$$\begin{bmatrix} X_l \\ Y_l \\ Z_l \end{bmatrix} = \begin{bmatrix} X_r & X_g & X_b \\ Y_r & Y_g & Y_b \\ Z_r & Z_g & Z_b \end{bmatrix} \begin{bmatrix} R \\ G \\ B \end{bmatrix} \tag{8}$$

To find the inputs α_is on the multi-spectral display (MSD) for the same spectrum $l(\lambda)$ we minimize our objective function (Equation 7) as explained in Section 3.2. Next, we display the spectrum on both of these displays using the computed input values. Once the temperature of lamps stabilized after 10 minutes of operation, we measure the displayed spectrum using a SOC-730 hyper-spectral camera. Let the measured spectrums from the MSD and CD be $l_M(\lambda)$

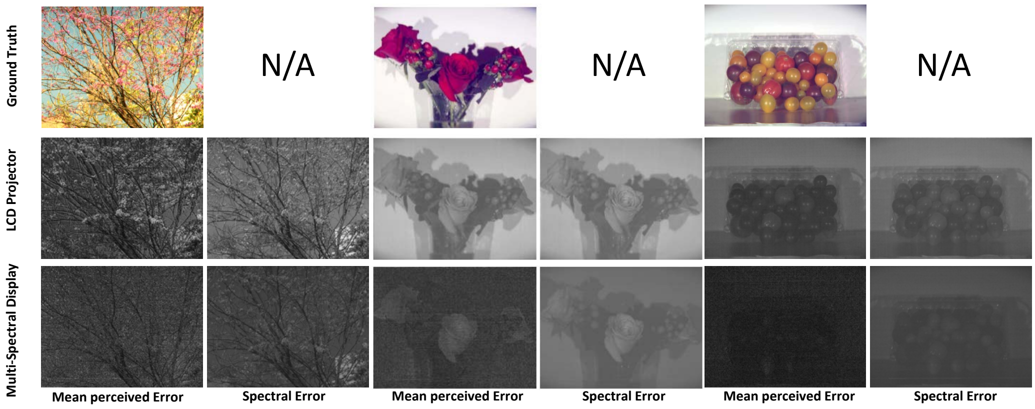

Figure 8: Examples of comparison between desired color image and perceived color image among 53 individual observers for three images (from left to right). For each image, we show the ground truth (top), the mean perceived error(left) and spectral error (right) when using the lcd (middle) and the multi-spectral display (bottom).

and $l_C(\lambda)$ respectively. Then we consider the sensitivities of the three sensors of a given observer denoted by $r_o(\lambda)$, $g_o(\lambda)$ and $b_o(\lambda)$. The response I_a evoked in a observer by an arbitrary spectrum $a(\lambda)$ is given by $I_a = (R_a, G_a, B_a) = (\int_\lambda a(\lambda) r_o(\lambda) d\lambda, \int_\lambda a(\lambda) g_o(\lambda) d\lambda, \int_\lambda a(\lambda) b_o(\lambda) d\lambda)$ respectively. We use this formula to find the response I_l, I_{l_M} and I_{l_C} evoked in an observer by ground truth or desired specturm $l(\lambda)$, and the measured $l_M(\lambda)$ and $l_C(\lambda)$ respectively. The L-2 distances of I_{l_M} and I_{l_C} from I_l give us the measure of the deviation of the perception created by the reproduced spectrum from the perception created by the ground truth or desired spectrum.

We use this method to compare the reproduction of a large number of spectra on our MSD prototype with that on an LCD projector (Epson EMP-74). We use our dataset of 60 hyperspectral images and the Stiles Burch Database of response of 53 varied human observers `www.cvrl.org` and find the deviation from ground truth at every pixel of the image from ground truth for every observer. The mean of these deviations and spectral error at every pixel are computed and visualized as an appropriately normalized grayscale image. These images are computed for both the MSD and the CD and compared, as shown in Figure 8. As is evident from the results, the MSD provides a much closer match to the perception of the ground truth than the conventional display. More results are shown in the video.

Comparison with other conventional displays: Due to instrumentation limitations, the method used for comparing LCD projectors cannot be used to compare our MSD to other conventional displays like laser or DLP projectors. Hyperspectal image acquisition is not possible on these displays since the images change temporally during the long exposure capture from the scanning based spectroradiometer. Hence, for these kinds of displays, we find the spectra of the primary of the projectors from factory specification sheets and simulate the response they will generate to a ground truth spectrum using the same aforementioned method. From this we can compute the spectral approximation projected by each of these displays and find the deviation from the ground truth spectrum. We use the data set of 2538 spectra which are acquired by using D65 standard illumination, an artificial mercury light (spiky spectrum) from `http://www.uef.fi/fi/spectral/artificial-lights` and 1269 Munsell reflectance spectra from `http://www.uef.fi/fi/spectral/munsell-colors-matt-spectrofotometer-measured`. We use the Stiles Burch Database of response of 53 varied observers and find the error in spectral approximation when the 2538 ground truth spectra were displayed on a LCD (Epson EMP-74), DLP (Optoma ML500) and laser (Microvision SHOWWX) projectors. We also simulate the results of a previous multi-primary display (MPD) method [YTO*02] using three long-pass filters (480nm, 580nm, 640nm), three short-pass filters (440nm, 520nm, 610nm) and three band-pass filters (440-480nm, 520-580nm, 610-640nm). The MPD method calculates the input value of each primary by minimizing the perceived error of CIE standard observer. The deviations are then averaged across all the different spectra and all different Stile-Burch observers to find the average deviation for each kind of display as shown in Table 3. This is compared with the deviation of response evoke by a CIE 1964 standard observer. Note that in both cases the MSD display yields the minimum error showing the benefits of a superior spectral reproduction. The MPD method shows less errors than our MSD method for the CIE 1964 observer, but it shows significantly higher Stiles Burch observer and error. This is expected since the MSD method is geared towards reducing standard observer error while observer metamerism stems from inaccurate spectral match.

5. Discussion

Light Throughput: Since each primary takes care of different ranges of wavelengths and the sum of all primaries

	Error					
	CIE 1964 Obsever		Stiles-Burch Obsever		Spectral Difference	
	mean	std	mean	std	mean	std
MSD	0.02	0.02	1.10	0.83	24.51	19.67
MPD	0.01	0.01	7.39	3.49	83.32	85.79
LCD	1.89	6.95	6.87	3.43	79.25	81.43
DLP	1.31	4.46	18.2	6.79	121.34	135.86
Laser	0.15	1.05	23.4	7.91	201.49	189.03

Table 3: Perceptual color difference $\triangle E_{Lab}$ of CIE standard observer and Stiles-Burch observer between desired color and simulated color for multi-spectral display(MSD), multi-primary display (MPD) [YTO*02], LCD display, DLP display and Laser display.

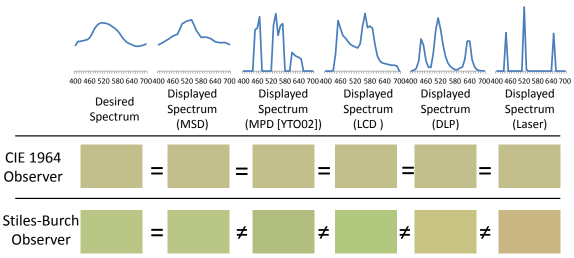

Figure 9: The ground truth spectrum number 540 in the data set of 2538 spectrum along with its reproduction on the different conventional displays as measured by a SOC-730 hyperspectral camera (top row). Note that these are all metameric spectrums with respect to the CIE 1964 standard observer and hence creates matching perception (middle row). However, when varied Stiles Burch observers are considered, the perception differ significantly across different displays due to inaccurate spectral reproduction. The color patches are real simulation results.

covers the entire range of visible wavelengths due to the complete coverage guideline, the total light throughput of the three projectors system is approximately equal to the light throughput of an unmodified projector when approximating the desired spectra by preserving the spectral shape.

Flicker in Multi-video Display: Our current implementation renders the multi-spectral images at a near interactive rate. With improved computing power and hardware, interactive multi-spectral video display is possible. However, the normalization step in our algorithm may introduce flicker in video display. Using normalization across multiple frames with max intensity prediction (e.g. Kalman filtering) may help to reduce flicker while a deeper investigation is still required.

Super-imposed Projection: The superimposing projection is not coaxial, which result in out-of-focus blur in the display. In addition, the warping of projected images may decrease the resolution of final display. Increasing the projection distance can alleviate the problem but at a compromised brightness.

Single Projector Display: Using multiple projectors is expensive and inflexible. Inspired by optical methods to make multiple smaller copies of an image from a projector using a multi-lens ensemble [SGM12, MRK*13], we would like to implement a single projector multi-spectral display by modifying the primaries for each copy. The prototype can be achieved by inserting filters (price: \$ 9) right before the multi-lens ensemble on the optical path, in such a manner that the copy created by each lens uses a different primary. We plan to use a 2×2 lens array (less than \$ 100) thus creating $3 \times 2^2 = 12$ primaries that is sufficient to construct a high quality multi-spectral display. Although resolution of final display will be compromised by a factor of $2^2 = 4$ compared to original display. This will still be at least 1 to 2 time higher than the spatial resolution currently available in multi-spectral images.

Heuristic Selection: Although our primary selection method can provide a relatively good set of primaries in a few milliseconds, the selection is based on a greedy heuristic method, therefore it cannot guarantee the optimal primary combination. In the future, we would like to design an objective function to find a content-independent optimal combination of primaries in an acceptable time using global search methods (e.g. genetic algorithm).

Extending to Channel Selection in Multi-spectral Imaging: Since multi-spectral recovery is a dual problem of multi-spectral approximation, we will explore and extend the primary selection method to select 'representative' channels in multi-spectral imaging. Both of these open up possibilities of designing projector and camera hardware that can achieve multi-spectral operations being within the commodity price range. In the future, we want to explore associated aspects like hardware design, illumination design, sensor mosaicing and demosaicing methods to gauge the extent to which our method can be exploited to create superior commodity capture and display devices.

6. Summary

In summary, we present a set of techniques and optimizations to enable appropriate filter selection for designing a content-independent multi-spectral display that guarantees both a good spectral reproduction and a large gamut. We show that our content-independent multi-spectral display can produce better perception and less observer metamerism than conventional displays. This enables us to provide high color-fidelity display and edit appearance of heritage and artworks realistically for various observers.

7. Acknowledgement

The work is partly supported by NSF IIS 0846144, the National Key Technology R&D Program projects (2012BAH43F05), National Basic Research Program of China (No. 2012CB725305) and Provincial Natural Science Foundation of Zhejiang (LY13F020050),.

References

[AF97] ALFVIN R., FAIRCHILD M.: Observer variability in metameric color matches using color reproduction media. *Color Research & Application 22*, 3 (1997), 174–188. 2

[AOYO99] AJITO T., OBI T., YAMAGUCHI M., OHYAMA N.: Multiprimary color display for liquid crystal display projectors using diffraction grating. *Optical Engineering 38*, 11 (1999), 1883–1888. 3

[AOYO00] AJITO T., OBI T., YAMAGUCHI M., OHYAMA N.: Expanded color gamut reproduced by six-primary projection display. In *Proceedings of SPIE - The International Society for Optical Engineering* (2000), vol. 3954, pp. 130–137. 3

[BCE07] BEN-CHORIN M., ELIAC D.: Multi-primary design of spectrally accurate displays. *Journal of the Society for Information Display 15*, 9 (2007), 667–677. 3

[BJ97] BRO R., JONG S. D.: A fast non-negativity-constrained least squares algorithm. *Journal of Chemometrics 11*, 5 (1997), 393–401. 7

[BJ04] BACH F. R., JORDAN M. I.: Learning spectral clustering. *Advances in Neural Information Processing Systems 16* (2004), 305–312. 5

[BL07] BRILL M. H., LARIMER J.: Metamerism and multi-primary displays. *Information Display 23*, 7 (2007), 16–21. 2

[CCO00] CHIAO C.-C., CRONIN T. W., OSORIO D.: Color signals in natural scenes: Characteristics of reflectance spectra and effects of natural illuminants. *Journal of the Optical Society of America A 17*, 2 (2000), 218–224. 5, 8

[CYBE10] CHI C., YOO H., BEN-EZRA M.: Multi-spectral imaging by optimized wide band illumination. *International Journal of Computer Vision 86*, 2-3 (2010), 140–151. 8

[Dan92] DANNEMILLER J. L.: Spectral reflectance of natural objects: How many basis functions are necessary? *Journal of the Optical Society of America A 9*, 4 (1992), 507–515. 4, 8

[DYA*12] DANIEL G. A., YU H., ALVIN L., SAJADI B., MAJUMDER A.: Fast high-resolution appearance editing using superimposed projections. *ACM Transactions on Graphics 31*, 2 (2012). 8

[FW07] FAIRCHILD M., WYBLE D.: Mean observer metamerism and the selection of display primaries. In *Color and Imaging Conference* (2007), pp. 151–156. 2

[IIN*01] ISHIHARA K., ISHIHARA S., NAGAMACHI M., HIRAMATSU S., OSAKI H.: Age-related decline in color perception and difficulties with daily activities measurement, questionnaire, optical and computer-graphics simulation studies. *International Journal of Industrial Ergonomics 28*, 3-4 (2001), 153–163. 2

[IRB02] IMAI F., ROSEN M., BERNS R.: Comparative study of metrics for spectral match quality. In *Conference on Colour in Graphics, Imaging, and Vision* (2002), vol. 1, pp. 492–496. 5

[KR04] KUEHNI R. G., RAMANATH R.: Comparing observers. *Color Research & Application 29*, 3 (2004), 183–186. 2

[LF11] LONG D., FAIRCHILD M.: Optimizing spectral color reproduction in multiprimary digital projection. In *19th Color and Imaging Conference* (2011), pp. 290–297. 3

[MRK*13] MANAKOV A., RESTREPO J. F., KLEHM O., HEGEDÜS R., EISEMANN E., SEIDEL H.-P., IHRKE I.: A reconfigurable camera add-on for high dynamic range, multi-spectral, polarization, and light-field imaging. *ACM Transactions on Graphics 32*, 4 (2013), 47:1–47:14. 11

[MRT08] MOHAN A., RASKAR R., TUMBLIN J.: Agile spectrum imaging: Programmable wavelength modulation for cameras and projectors. *Computer Graphics Forum 27*, 2 (2008), 709–717. 3

[MWDG13] MASIA B., WETZSTEIN G., DIDYK P., GUTIERREZ D.: A survey on computational displays: Pushing the boundaries of optics, computation, and perception. *Computer & Graphics 37*, 8 (2013), 1012–1038. 3

[PMaH97] POZA A. J., MARTINEZ J. A., ANDE. HITA M. M.: A 2° standard deviate observer from the 1955 Stiles-Burch dataset. *Journal of Optics 28*, 1 (1997), 20–25. 7, 9

[Ram09] RAMANATH R.: Minimizing observer metamerism in display systems. *Color Research & Application 34*, 5 (2009), 391–398. 4

[RBA*12] RICE J. P., BROWN S. W., ALLEN D. W., YOON H. W., LITORJA M., HWANG J. C.: Hyperspectral image projector applications. In *SPIE MOEMS-MEMS* (2012), International Society for Optics and Photonics, pp. 82540R–82540R. 3

[RC05] ROTH S., CALDWELL W.: Four orimary color projection display. *SID Symposium Digest of Technical Papers 36* (2005), 1818–1821. 3

[RPSF14] RODRIGUEZ-PARDO CARLOS E., SHARMA G., FENG X.-F.: Primary selection for uniform display response. In *Color Imaging XIX: Displaying, Processing, Hardcopy, and Applications* (2014), vol. 9015, pp. 90150I–90150I–9. 3

[SB59] STILES W. S., BURCH J. M.: N.P.L. colour-matching investigation: Final report. *Optica Acta: International Journal of Optics 6*, 1 (1959), 1–26. 2

[SGM12] SAJADI B., GOPI M., MAJUMDER A.: Edge-guided resolution enhancement in projectors via optical oixel sharing. *ACM Transactions on Graphics 31*, 4 (2012), 79:1–79:10. 11

[SLGM09] SAJADI B., LAZAROV M., GOPI M., MAJUMDER A.: Color seamlessness in multi-projector displays using constrained gamut morphing. *IEEE Transactions on Visualization and Computer Graphics 15*, 6 (2009), 1317–1326. 8

[SM09] SAJADI B., MAJUMDER A.: Markerless view-independent registration of multiple distorted projectors on extruded surfaces using an uncalibrated camera. *IEEE Transactions on Visualization and Computer Graphics 15*, 6 (2009), 1307–1316. 8

[SM10] SAJADI B., MAJUMDER A.: Auto-calibration of cylindrical multi-projector systems. In *IEEE Virtual Reality Conference* (2010), pp. 155–162. 8

[SM11] SAJADI B., MAJUMDER A.: Automatic registration of multi-projector domes using a single uncalibrated camera. *Computer Graphics Forum 30*, 3 (2011), 1161–1170. 8

[SSM01] SUKTHANKAR R., STOCKTON R. G., MULLIN M. D.: Smarter presentations: Exploiting homography in camera-projector systems. In *Eighth IEEE International Conference on Computer Vision, ICCV 2001.* (2001), vol. 1, pp. 247–253. 8

[TMGR10] THOMPSON D. R., MANDRAKE L., GILMORE M. S., R.CASTANO: Superpixel endmember detection. *IEEE Transactions on Geoscience and Remote Sensing 48*, 11 (2010), 4023–4033. 4, 5

[TYN*12] TERAGAWA M., YOSHIYAMA K., NAKAGAWA S., TOMIZAWA K., YOSHIDA Y.: Review paper: Multi-primary-color displays: The latest technologies and their benefits. *Journal of the Society for Information Display 20*, 1 (2012), 1–11. 3

[YTO*02] YAMAGUCHI M., TERAJI T., OHSAWA K., UCHIYAMA T., MOTOMURA H., MURAKAMI Y., OHYAMA N.: Color image reproduction based on the multispectral and multiprimary imaging: Experimental evaluation. *Electronic Imaging 4663* (2002), 15–26. 3, 10, 11